



Formulation of Novel Boswellic Acid Loaded-PEGlyated Nanoparticles and Effect on SARS COVID 19 Virus: *in silico* Docking Analysis and ADMET Studies

SNEHA THAKUR^{1,*} and M. KIRANMAI²

¹Department of Pharmacognosy, St. Pauls College of Pharmacy, Turkayamjal-501510, India

²Department of Pharmaceutical Chemistry, St. Pauls College of Pharmacy, Turkayamjal-501510, India

*Corresponding author: E-mail: snehathakur2189@gmail.com

Received: 15 January 2024;

Accepted: 15 May 2024;

Published online: 31 May 2024;

AJC-21656

SARS COVID-19 virus is serious threats to the mankind changing its virulence. The pandemic emergence resulted in the change of health care scenario since its outbreak and suggested the inclusion of molecular modeling and combinatorial chemistry process that hastens the drug discovery process resulting in screening of large number of compounds for the therapeutic target proposed. The studies revealed that the boswellic acid (pentacyclic triterpenoid) obtained from gum resin of *Boswellia serrata* is found to have potential against the SARS covid virus. The present study was conducted to synthesize boswellic acid-PEG from isolated boswellic acid (gum resin of *B. serrata*) and evaluated the anti-covid potential of boswellic acid by *in silico* docking studies and toxicity analysis by ADMET Pro. The target protein PDB RNA polymerase (1S76), protease (6LU7), ACE2 (6M0J) were downloaded from RCDB database. The boswellic acid was active against the selected target proteins active for SARS virus entry into the cells and also prevent the viral multiplication. ADMET studies have proved slight endo-carcinogenicity, which increases with dose. Thus, this novel molecule can be developed as lead against the SARS virus by formulating boswellic acid-PEG nanoparticles with sustained release characteristics. As an attempt to develop the drug boswellic acid-PEG nanoparticles with PEG as permeation enhancer for oral drug delivery was performed and characterized using DLS, FTIR, XRD and SEM techniques, which has proven the 253 nm size, stable, highly dispersed, spherical shape without any agglomeration. The drug release studies proved the sustained release nature of the nanoparticles, which leads to reduce dosage. Further, *in vivo-in vitro* correlation proves the clinical validation for drug discovery process.

Keywords: SARS COVID 19 virus, Boswellic acid, Nanoparticles, *in silico*, Drug release' ADMET.

INTRODUCTION

The *in silico* docking studies offer a great advantage to analyze structure, physico-chemical properties, solubility and ADMET profile which enables to focus to modify the lead in such a way to have enhanced action, thereby reducing the burden of time and effort [1]. Much of the identified leads were screened initially for the potential of the compound at the receptor level using molecular modeling studies. The affinity, binding capacity, physico-chemical nature and ADMET (absorption, distribution, metabolism, excretion, toxicity) are the prime requisites that motivate the research studies for the lead identification and later transformation [2] into a drug delivery system. The COVID-19 pandemic was envisaged with strict lockdown which could halt the research for a while. There were no many testing methods available to screen the drugs [3], which was

better handled by the use of *in silico* docking techniques that could estimate huge number of leads which were screened with advanced molecular modeling techniques. The phytochemical leads once identified could be estimated for their potency based on affinity and solubility with least toxicity.

The phytochemicals derived from *Tinospora cardifolia*, *Ocimum*, *Curcuma*, *Panax*, *Mentha* are promising to combat the infection. The challenges thrown by the covid-19 pandemic shook the countries with alarming rates of mortality globally. Several covid issues [4,5] have been addressed with antibiotics and antiviral agents along with diet with enriched nutrients was the only treatment. The antiviral drugs in covid-19 were used in combination with other antibiotics which on long term use have shown side effects but could not address the infection as single point. The COVID-19 virus is more resistant to drugs because it may enter the body by multiple entrance points, such

as protease (protein denaturation), ACE-2 (organ inflammation) and RNA polymerase (conversion and multiplication) [6,7]. These observations lead to multiple drug therapy. The SARS covid infection still is a point of research interest and much needed intervention to be handled to save the globe.

Many phytochemicals derived from the plants face the challenges in the drug derivatization process due to hindrance of its solubility and bioavailability [8,9]. The recent advances in the nanotechnology focus the modulation of drug entry barriers to make phytochemicals modulated with enhanced solubility and bioavailability [10,11]. Current research is focused more on deriving phytomolecules with potent anti-SARS viral activity with improved bioavailability and solubility. Boswellic acid [12,13] is obtained from the plant resin of *Boswellia serrata*, which is used in treating osteoarthritis, crohns disease, inflammatory bowel disease, *etc.* Boswellic acid was found to have huge dose with limited solubility and bioavailability. Thus, observing the potential of boswellic acid [14-17] as widely pharmacologically active agent, the present research focused to repurpose the boswellic acid as anticovid agent and further overcome its toxicity, dose related side effects and modify the drug into PEG nanoparticles with improved solubility and bioavailability.

Polyethylene glycols (PEGs) are used as natural hydrophilic polymers in several cosmetics and also as excipient in wide pharmacological products due to its safety [18-21]. The literature supports no data on the improved activity of boswellic acid-PEG nanoparticles as anti-covid agent. The novelty of the present research lies in the synthesis of boswellic acid-PEG nanoparticles as formulation against the covid-19 infection. Thus, the research study conducted could prove the novel boswellic acid-PEG nanoparticles as effective against covid-19 virus.

EXPERIMENTAL

Boswellic acid, polyethylene glycol (PEG), ethanol were obtained from Sigma-Aldrich Chemicals, India. Melting points of boswellic acid were recorded on open capillary Buchi instrument and are uncorrected. The FTIR spectra were recorded on a Perkin-Elmer FT-IR 240-C spectrometer using KBr pellet method. The isolated compound was identified by TLC monitored on silica gel percolated plates of Merck and the spots were visualized with ethyl acetate and hexane as mobile phase solvent (30:70). The silica gel (100-200 mesh) used for column chromatography was procured from Merck Ltd., India.

Extraction and isolation: The plant gum resin of *Boswellia serrata* was used for the extraction. Approximate 100 g of resin was loaded into Soxhlet apparatus with hexane and methanol simultaneously. Based on preliminary qualitative screening, the methanol extract was found to be high with boswellic acid [14,16]. Further column was loaded with silica gel (125-250 grade) and extracted. Then eluted with hexane initially to remove non-polar impurities and further using ethyl acetate and hexane as mobile phase combinations, which yielded boswellic acid in 40-50% ethyl acetate fractions. The isolated boswellic acid was found to be mixture identified using UV, HPLC, FTIR

and TLC studies, which could prove that boswellic acid is 99% pure. Boswellic acid was used for synthesis of facile green boswellic acid PEG nanoparticles with improved penetration ability using PEG.

Preparation of PEGlyated boswellic acid nanoparticles: The PEGlyated boswellic acid nanoparticles were prepared using desolvation procedure with little modification. Boswellic acid (100 mg) was dissolved in 20 mL of ethanol (95%) with constant magnetic stirring for 10 min at room temperature followed by the addition of 20 mL of purified water. The solution was concentrated to get nanosuspension on a rotavapour. The nanosuspension was further added with PEG polymer solution prepared by dissolving the polymer in water and to yield stable nanoparticles. The polymer solution was added in three ratio, which resulted in the synthesis of PEGlyated boswellic acid nanoparticles [19-21]. The obtained nanoparticles were characterized by UV-HPLC, FTIR, SEM, DLS and XRD techniques.

Drug loading capacity: The drug loading capacity was studied at room temperature at pH 3 in ethanol. Boswellic acid-PEG nanoparticles (10 mg) were dispersed in 5 mL of ethanol, agitated for 48 h and then centrifuged. The collected filtrate and analyzed by UV spectrophotometer (Shimadzu) to determine drug loading capacity (eqn. 1) and further analyzed through Minitab free software trial [22-24].

$$\text{Drug loading capacity (\%)} = \frac{\text{Weight of the drug in nanoparticles}}{\text{Weight of the nanoparticles}} \times 100$$

Drug release studies: The calibration curve was plotted by taking series of concentrations and the curve was plotted at maximum wavelength obtained. The *in vitro* drug release [25] was evaluated using USP dissolution apparatus I basket type to evaluate the drug release from PEG nanoparticles. The USP dissolution apparatus I is a rotating basket type apparatus with cylindrical glass vessel of hemispherical bottom with 1 L capacity which was partially immersed in water bath main-tained at 37 ± 2 °C. The cylindrical basket made of 22 mesh size holds the sample. The sample of weighed quantity was packed in cotton muslin cloth and kept inside the basket. All metal parts were made up of SS16 grade and the basket was rotated at variable speed. The phosphate buffer saline (pH 7.4) was taken in the dissolution vessel (900 mL) being stirred at 100 rpm maintained in sink conditions. The withdrawn samples were analyzed by the UV-visible spectrophotometer at 249 nm [26]. The results of drug release were fitted into drug release kinetic models and respective graphs were obtained using Design Expert 12.0. The kinetics were evaluated to understand the nature of drug release.

Docking studies: Boswellic acid was screened for the anti-covid viral activity using the molecular docking analysis with Autodock 4.0 software [27-31]. The proteins with PDB IDs *i.e.* RNA polymerase (PDB_ID: 1S76), COVID-19 main protease (PDB_ID: 6LU7) were downloaded from the RCDB database. The boswellic acid structure was downloaded from the PubChem Database. The docking study involved three main steps, which include the preparation of ligand, protein and finally docked. Molecular docking study of boswellic acid was carried out using Autodock software. Docking of the compound was carried out on RNA polymerase (PDB_ID: 1S76), COVID-

19 main protease (PDB_ID: 6LU7) and SARS-CoV-2 spike receptor-binding domain bound with ACE2 (PDB_ID: 6M0J) proteins. These proteins were retrieved from protein data bank. During the docking, we have used grid box parameters for RNA polymerase as grid centre: $x = -44.43$, $y = 11.601$, $z = 42.411$ and grid box size: $x = 58$, $y = 50$, $z = 50$. The grid box parameters for COVID-19 main protease were used as grid centre: $x = 9.937$, $y = 14.655$, $z = 67.125$ and grid box size: $x = 50$, $y = 62$, $z = 40$. Further, for ACE2 grid box parameters were used as grid centre: $x = 25965$, $y = 7.317$, $z = 33.049$ and grid box size: $x = 50$, $y = 48$, $z = 46$. For all proteins, the grid spacing was used as 0375 Å and for each docking, we generated 10 conformations. Input preparation carried out using MGL tools-1.5.6 and the results were analyzed using Autodock Tools and Pymol software.

***In silico* bioavailability and drug likeness screening:**

The chemical descriptors for the pharmacokinetics properties were calculated to check the compliance of studied compound with the standard range. For this the aqueous solubility, blood brain barrier penetration, cytochrome P450 2D6 binding, hepatotoxicity, intestinal absorption and plasma protein binding were calculated [32]. The calculation of these chemical properties was intended as the first step toward analyzing the novel chemical entities, in order to check the failure of lead candidates which may cause toxicity or metabolized by the body in to an inactive form or one unable to cross the intestinal membranes. The pharmacokinetic profiles of all the compounds under investigation were predicted by means of six pre-calculated ADMET models. The aqueous solubility prediction (defined in water at 25 °C) indicated that all the compounds are soluble in water. The compounds are found to be non-inhibitors of cytochrome P450 2D6 (CYP2D6). The CYP2D6 enzyme is one of the important enzymes involved in drug metabolism.

ADMET prediction: The ADMET studies which predict the toxicity [31] were estimated by the software ADMET pro (Version 6.0). To understand the toxicity risk in different areas *i.e.* skin irritancy, ocular irritancy, aerobic biodegradability, mutagenicity, endocarcinogenicity and developmental potential for toxicity should be checked the safety of the compounds, which is crucial for a successful drug. All the compounds were found to be non-mutagenic and either mild or no irritancy (ocular & skin) when compared to doxorubicin which is mutagenic and acarbose, which shows severe ocular irritancy. The dose dependent toxicity such as carcinogenic potency TD_{50} , rat inhalational LC_{50} , rat oral LD_{50} , daphnia EC_{50} (mg/L), rat maximum tolerated dose feed, rat chronic LOAEL in lieu with the effective concentration extent are studied.

RESULTS AND DISCUSSION

Boswellic acid was formulated into nanoparticles using desolvation procedure using PEG 35000 as co-solvent. Further, the boswellic acid nanoparticles were characterized for stability, particles size, agglomeration and crystalline nature using DLS, FTIR and XRD spectrometric studies. The melting point of boswellic acid was found to be 123.6 °C, whereas boswellic acid-PEG nanoparticles was found to be 148.9 °C.

Docking analysis: The binding affinity of boswellic acid with RNA polymerase, main protease and ACE2 with its surrounded amino acid residues were analyzed using molecular docking studies. Boswellic acid showed strong interaction with three COVID-19 targets with good docking score (Table-1).

The interactions of boswellic acid in the active site of RNA polymerase protein are depicted in Fig. 1a. Boswellic acid is stabilized by hydrogen bonds with Asp-812, Lys-631 and Cys-540 residues in the active site. The molecule also showed hydrophobic interactions with Asp-537, Ser-539 and His-463

TABLE-1
PROTEIN LIGAND BINDING INTERACTION ENERGIES (kcal/mol) CALCULATED BY USING AUTODOCK
(Details of LibDock score, hydrogen bonds, Pi interactions and active site pocket residues by molecular docking studies)

Compound	Target PDBID	Docking score (Kcal/mol)	Active site amino acids	H bond	Affinity with amino acids
Boswellic acid	1S76	-7.8	Asp-812, Lys-631, Cys-540, Asp-537, Ser-539, His-463	3	Asp-812, Lys-631, Cys-540,
	6LU7	-6.8	Asn-142, His164, His-41, Thr-25, Thr-26, Met-49, Cys-145	2	Asn-142, His164
	6M0J	-8.0	Asn-149, Trp-271, Asp-269, Phe-274, Tyr127	1	Asn-149

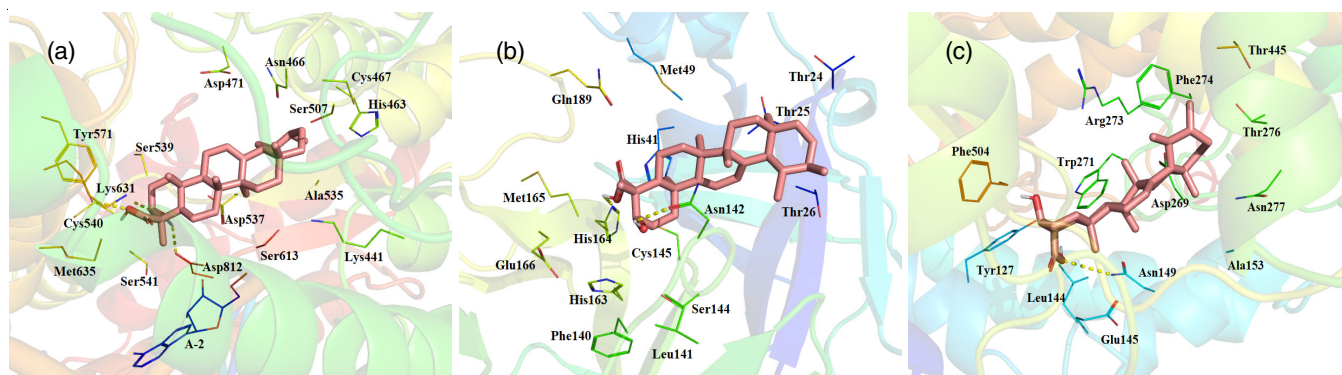


Fig. 1. Molecule boswellic acid docked in the active site of the (a) RNA polymerase (PDB_ID: 1S76); (b) main protease (PDB_ID: 6LU7) and (c) active site of the ACE2 (PDB_ID: 6M0J). Inhibitor molecule shown in stick style and the active site amino acid side residues are shown in line style

residues in the active site. Fig. 1b depicts the interactions of boswellic acid in the active site of main protease. The ligand molecule is stabilized by hydrogen bonds with Asn-142 and His164 residues in the active site. The ligand also showed hydrophobic interactions with His-41, Thr-25, Thr-26, Met-49 and Cys-145 residues in the active site. Fig. 1c shows the interactions of boswellic acid in the active site of ACE2 and the lead molecule is stabilized by hydrogen bond with Asn-149 and also showed hydrophobic interactions with Trp-271, Asp-269, Phe-274 and Tyr127 residues in the active site.

The docking studies could prove the potential of boswellic acid has strong affinity towards the COVID proteins binding site and has effectively inhibited the SARS covid proteins. The repurposing of boswellic acid was proven beneficial effectively, which ultimately resulted in determining the potency of boswellic acid as effective anticovid agent.

ADMET profile: During ADMET screening, the predictive carcinogenicity was observed. The candidate compound has high bounding with plasma proteins and also CYP inhibition (Tables 2 and 3).

TABLE-2
PREDICTIVE MOLECULAR
PROPERTIES OF BOSWELLIC ACID

Property	Value
Molecular weight	456.71
AlogP	7.09
H-Bond acceptor	2
H-Bond donor	2
Rotatable bonds	1
Molecular refractivity	136.91
Topological polar surface area	57.53
Water solubility	-3.787
Plasma protein binding	0.844
Acute oral toxicity	1.186 kg/mol
Tetrahymena pyriformis	0.064 pIGC ₅₀ (µg/L)

TABLE-3
ADMET PREDICTED PROFILE OF BOSWELLIC
ACID ALONG WITH THE TOXICITY PROFILE

Human intestinal absorption	0.9853
Blood brain barrier	0.5353
CYP2C9 substrate	0.8404
CYP2D6 substrate	0.8509
CYP3A4 inhibition	0.8579
CYP2C9 inhibition	0.8298
CYP2C19 inhibition	0.8660
CYP2D6 inhibition	0.9520
CYP1A2 inhibition	0.8659
CYP inhibitory promiscuity	0.9221
Carcinogenicity	0.9900
Eye irritation	0.9351
Eye corrosion	0.9900
Hepatotoxicity	0.7000
Reproductive toxicity	0.9222
Biodegradation	0.8500
Fish aquatic toxicity	0.9900
Immunotoxicity	0.9300

Values exceeds 0.7 are considered as the property can applicable for the molecule; The values calculate from ADMETSAR and Protox II tools.

Boswellic acid-PEG silver nanoparticles: The PEGylated-boswellic acid nanoparticles were characterized by UV, DLS, FTIR, SEM and XRD techniques. The UV-HPLC spectrum was obtained at 249 nm. The PEG was used to mask the hydrophobic character of the boswellic acid PEG nanoparticles, resulting in an improved hydrophilicity that was observed in the FTIR spectrum. The particle size was determined to be approximately 253 nm in the DLS experiments, which is an appropriate size for moderate bioavailability [33]. The zeta potential was found to be ≤ 30 mm, which is considered to be ideal for stability. The SEM studies have shown the spherical shape of the nanoparticles and the XRD studies have proven the crystalline nature of the PEGylated-boswellic acid nanoparticles (Fig. 2). The several broad Bragg peaks corresponds to 111, 200, 311, 331 orientations corresponding to 2θ values of 21.80°, 36.10°, 37.90° and 79.40°, respectively and these peaks precisely are indexed well in the Joint Committee on Powder Diffraction Standards (JCPDS card no. 61-1894).

FTIR analysis: The FTIR spectrum (Fig. 3) reported sharp peaks at range of 2945-2890 cm^{-1} , which indicates that there is a strong OH stretching [34]. The peak of 2949 cm^{-1} of C=C group and the peak of 1703 cm^{-1} of the carboxyl group. The bands at 1701 cm^{-1} indicates the strong C=O stretching and the aromatic groups can be detected in the region of 1200-1000 cm^{-1} . The methylene groups can be identified in the range of 900-800 cm^{-1} . The shift in vibrations due to the hydrophilic interactions of PEG were clearly reported in the FTIR, which proves the encapsulation and polymer binding of PEG with boswellic acid (Fig. 3b).

Drug release nature and loading capacity: The UV-vis studies were conducted [35] for the pure drug for λ_{max} and R^2 was found to be 0.983 at 249 nm. The standard calibration curve (Fig. 4) was plotted for concentration ranges of 20-100 mg/mL after serial dilution of stock (1 mg/mL). The purity of was found to be 98%. The studies on drug loading capacity have shown drug loading as Q ($\text{mg}^1 \text{g}^{-1}$) as 93.21%, which is considered to be ideal for enhanced bioavailability. Further the drug release kinetics have proven the sustained release nature of boswellic acid nanoparticles owed to the slow release nature and complexation between the pharmacophore boswellic acid and the PEG. The drug release was found to be 99.3% in 10 h and 97.2% in 24 h for PEGylated boswellic acid nanoparticles (Fig. 5, Table-4). The drug release kinetic models (Table-5) were established using Design Expert version 12.0 demonstrated that boswellic acid exhibits zero order kinetics with a R value ≤ 0.89 in the Higuchi model with Fick's diffusion. The PEGylated boswellic acid nanoparticles follow first order kinetics with R value ≥ 0.89 in Higuchi model which proves non-fickian diffusion and supercase II transport. Thus, the PEGylated boswellic acid nanoparticles can be suitably handled for the dose related endotoxicity of boswellic acid. The dissolution data was fitted in various kinetic models [36-42] such as zero-order, first order, Higuchi and Peppas models. Figs. 6 and 7 describe the release mechanism of PEGylated boswellic acid nanoparticles.

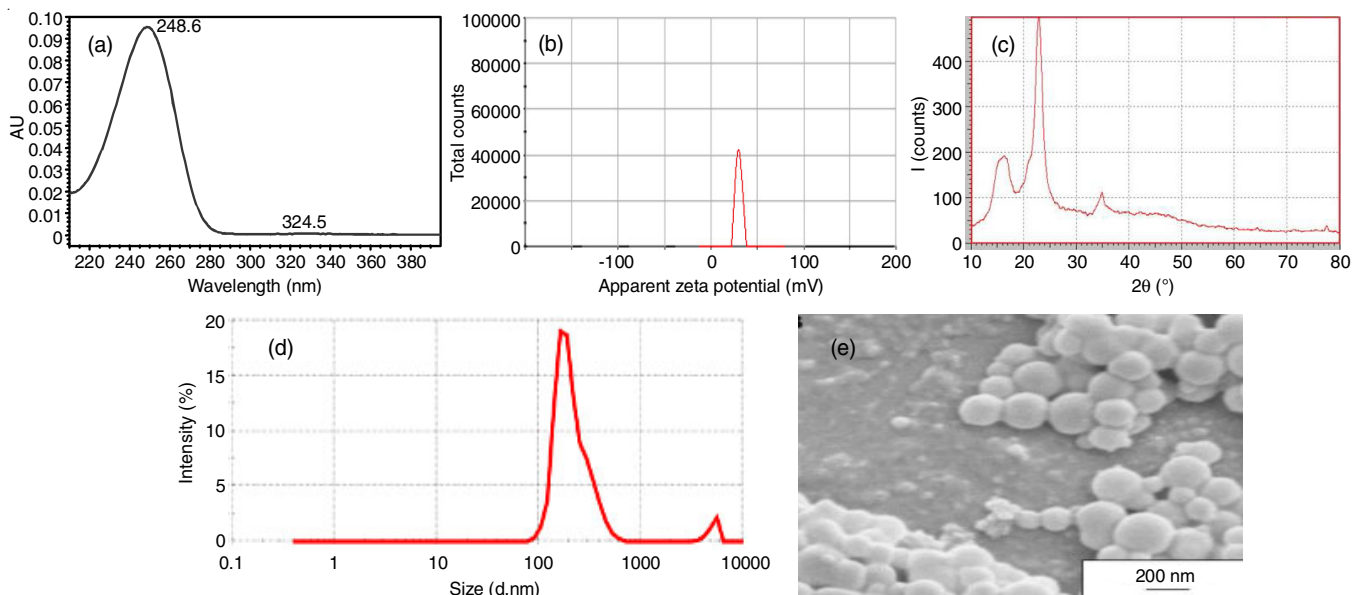


Fig. 2. Boswellic-PEG nanoparticles (a) UV_HPLC spectrum, (b) zeta potential of boswellic acid, (c) XRD graph, (d) particle size and (e) SEM

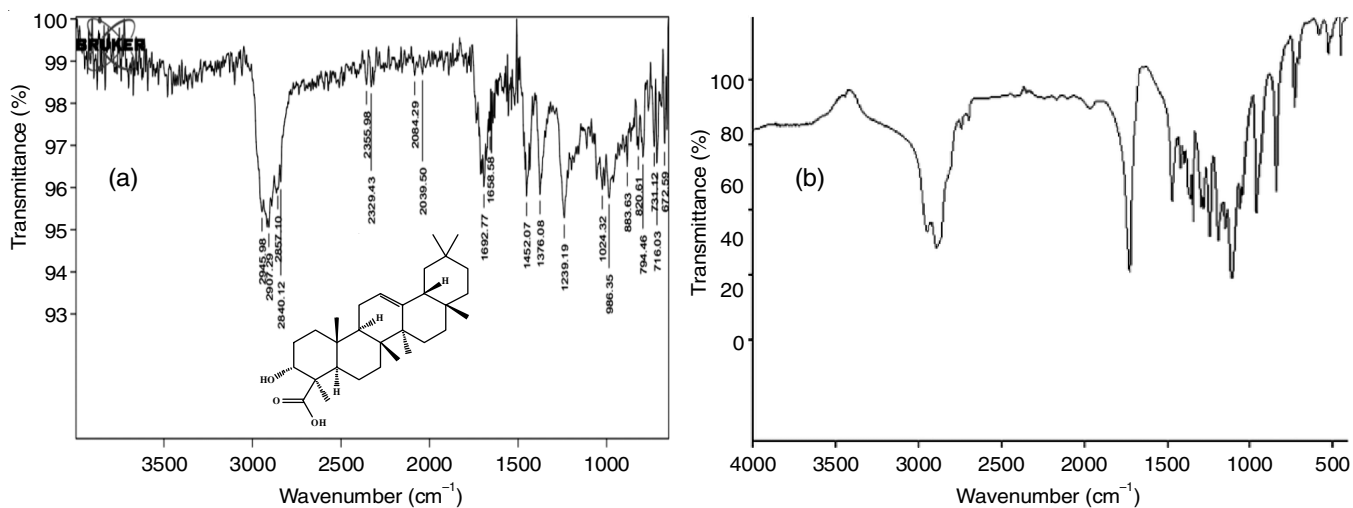


Fig. 3. FTIR spectrum (a) Boswellic acid (b) PEGylated boswellic acid nanoparticles

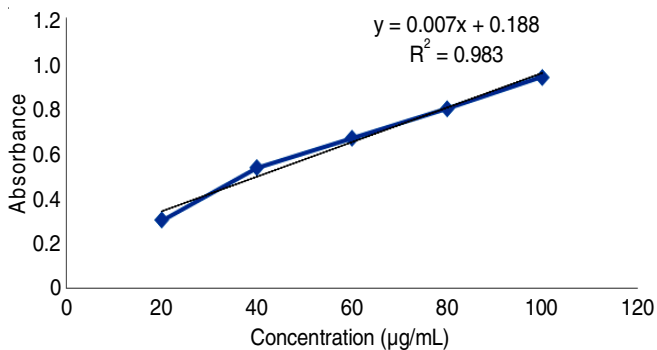


Fig. 4. Standard calibration curve for boswellic acid

TABLE-4 DRUG RELEASE STUDIES OF PEGylated BOSWELLIC ACID NANOPARTICLES AND BOSWELLIC ACID		
Time (h)	Percent drug release of Boswellic acid	Percent drug release of PEGylated Boswellic acid nanoparticles
0	0	0
0.5	31.3	24.6
1	56.7	33.8
2	62.9	55.3
4	77.3	64.0
6	89.5	74.9
8	99.3	86.3
10		93.7
12		95.3
24		97.2

Conclusion

Boswellic acid was isolated from the gum resin of plant *Boswellia serrata* by column chromatography in 40% ethyl acetate in hexane fraction, characterized TLC using 30% ethyl

acetate in hexane as mobile phase solvent and UV-HPLC at 249 nm. The *in silico* docking with Covid-19 protein targets

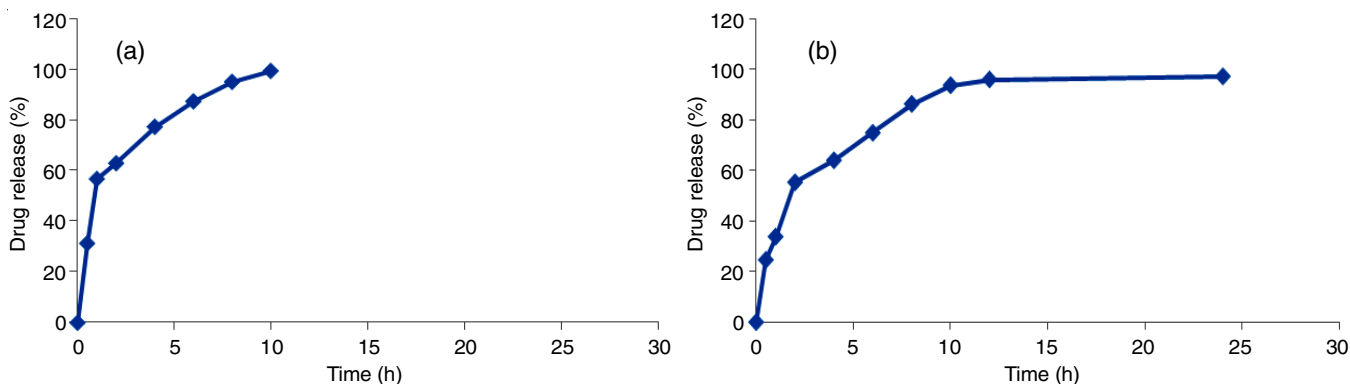


Fig. 5. *In vitro* drug release studies of (a) Boswellic acid (b) PEGylated Boswellic acid nanoparticles

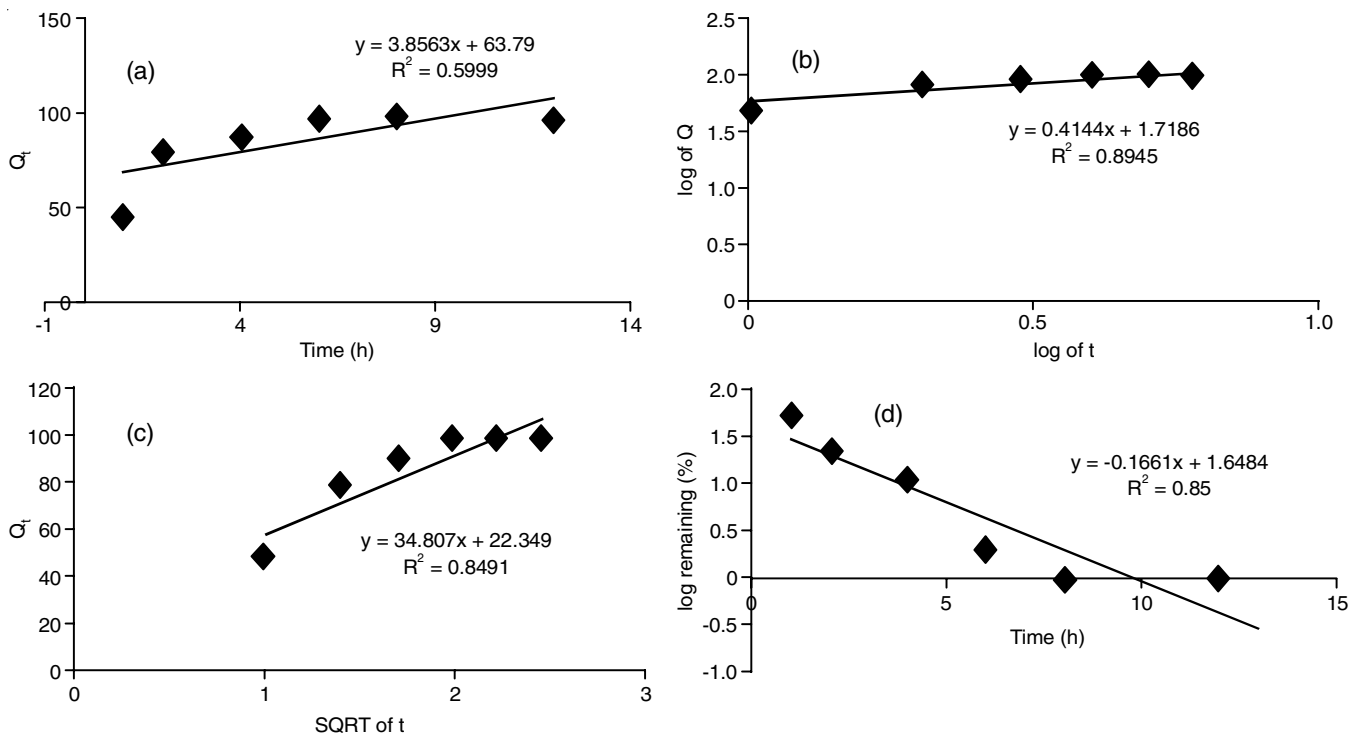


Fig. 6. Drug release kinetics of Boswellic acid (a) zero order, (b) Korsmeier-Peppas model, (c) Higuchi model and (d) first order

TABLE-5
DRUG RELEASE KINETICS OF BOSWELLIC ACID AND
PEGLYATED BOSWELLIC ACID NANOPARTICLES

Zero order	0.5990	0.8551
First order	0.8900	0.9774
Higuchi	0.8491	0.9432
Korsmeier Peppas	0.8945	0.9564

and the ADMET toxicity studies revealed high binding affinities and the drug is mild endocarcinogen with other toxicity within the limits as required in the drug discovery procedure. Further the dose related toxicity could be reduced by formulation of Boswellic acid-PEG nanoparticles which are novel and proven to be highly stable, dispersed and crystalline in nature. The hydrophobic nature of boswellic acid was masked and transformed to stable boswellic acid-PEG nanoparticles with average size of 253 nm, spherical, crystalline and enhanced bioavailability with sustained release nature. The *in vivo-in vitro* correl-

ation is essential to determine the lead component as a lead drug for the treatment of SARS-CoV-2 therapy.

ACKNOWLEDGEMENTS

The authors are thankful to Management of St. Pauls College of Pharmacy for the support and encouragement.

CONFLICT OF INTEREST

The authors declare that there is no conflict of interests regarding the publication of this article.

REFERENCES

1. Q. Li, *China CDC Wkly.*, **2**, 79 (2020); <https://doi.org/10.46234/ccdcw2020.022>
2. W. Tan, X. Zhao, X. Ma, W. Wang, P. Niu, W. Xu, G. F. Gao and G. Wu, *China CDC Wkly.*, **2**, 61 (2020); <https://doi.org/10.46234/ccdcw2020.017>

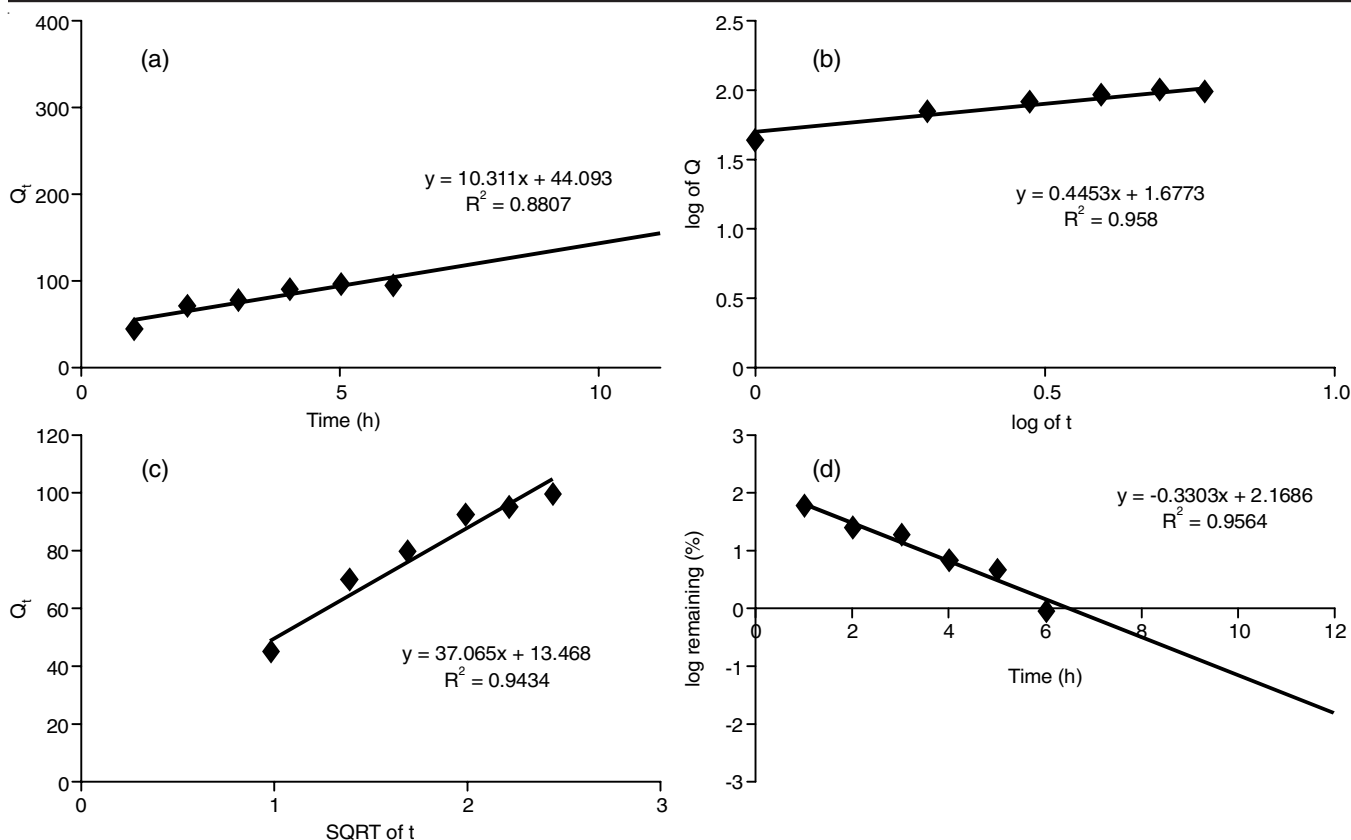


Fig. 7. Drug release kinetics of PEGlyated Boswellic acid nanoparticles (a) zero order, (b) Korsmeyer-Peppas model, (c) Higuchi model and (d) first order

3. N. Zhu, D. Zhang, W. Wang, X. Li, B. Yang, J. Song, X. Zhao, B. Huang, W. Shi, R. Lu, P. Niu, F. Zhan, X. Ma, D. Wang, W. Xu, G. Wu, G.F. Gao and W. Tan, *N. Engl. J. Med.*, **382**, 727 (2020); <https://doi.org/10.1056/NEJMoa2001017>
4. N. Xiang, F. Havers, T. Chen, Y. Song, W. Tu, L. Li, Y. Cao, B. Liu, L. Zhou, L. Meng, Z. Hong, R. Wang, Y. Niu, J. Yao, K. Liao, L. Jin, Y. Zhang, Q. Li, M.-A. Widdowson and Z. Feng, *Emerg. Infect. Dis.*, **19**, 1784 (2013); <https://doi.org/10.3201/eid1911.130865>
5. V.J. Munster, M. Koopmans, N. van Doremalen, D. van Riel and E. de Wit, *N. Engl. J. Med.*, **382**, 692 (2020); <https://doi.org/10.1056/NEJMp2000929>
6. L. Samavati and B.D. Uhal, *Front. Cell. Infect. Microbiol.*, **10**, 317 (2020); <https://doi.org/10.3389/fcimb.2020.00317>
7. E.I. Azhar, S.A. El-Kafrawy, S.A. Farraj, A.M. Hassan, M.S. Al-Saeed, A.M. Hashem and T.A. Madani, *N. Engl. J. Med.*, **370**, 2499 (2014); <https://doi.org/10.1056/NEJMoa1401505>
8. F. Aqil, R. Munagala, J. Jeyabalan and M.V. Vadhanam, *Cancer Lett.*, **334**, 133 (2013); <https://doi.org/10.1016/j.canlet.2013.02.032>
9. S. Kalepua and V. Nekkanti, *Acta Pharm. Sinica B*, **5**, 442 (2015); <https://doi.org/10.1016/j.apsb.2015.07.003>
10. C.T. Bauch, J.O. Lloyd-Smith, M.P. Coffee and A.P. Galvani, *Epidemiology*, **16**, 791 (2005); <https://doi.org/10.1097/01.ede.0000181633.80269.4c>
11. Y. Liu, Y. Liang, J. Yuhong, P. Xin, J.L. Han, Y. Du, X. Yu, R. Zhu, M. Zhang, W. Chen and Y. Ma, *Drug Des. Devel. Ther.*, **18**, 1469 (2024); <https://doi.org/10.2147/DDDT.S447496>
12. S. Perlman, *N. Engl. J. Med.*, **382**, 760 (2020); <https://doi.org/10.1056/NEJMMe2001126>
13. W. Sungnak, N. Huang, C. Bécavin, M. Berg, M. Litvinukova, R. Queen, C. Talavera-López, H. Maatz, D. Reichart, F. Sampaziotis, K.B. Worlock, M. Yoshida and J.L. Barnes, *Nat. Med.*, **26**, 681 (2020); <https://doi.org/10.1038/s41591-020-0868-6>
14. K. Reising, J. Meins, B. Bastian, G. Eckert, W.E. Mueller, M. Schubert-Zsilavec and M. Abdel-Tawab, *Anal. Chem.*, **77**, 6640 (2005); <https://doi.org/10.1021/ac0506478>
15. A.S. Shah, S.I. Rathod, N.B. Suhagia, S.S. Pandya and V.K. Parmar, *J. Chromatogr. Sci.*, **46**, 735 (2008); <https://doi.org/10.1093/chromsci/46.8.735>
16. A. Frank and M. Unger, *J. Chromatogr. A*, **1112**, 255 (2006); <https://doi.org/10.1016/j.chroma.2005.11.116>
17. N.K. Roy, D. Parama, K. Banik, D. Bordoloi, A.K. Devi, K.K. Thakur, G. Padmavathi, M. Shakibaei, L. Fan, G. Sethi and A.B. Kunnumakkara, *Int. J. Mol. Sci.*, **20**, 4101 (2019); <https://doi.org/10.3390/ijms20174101>
18. L.M. Ensign, C. Schneider, J.S. Suk, R. Cone and J. Hanes, *Adv. Mater.*, **24**, 3887 (2012); <https://doi.org/10.1002/adma.201201800>
19. S. Gaspani and B. Milani, *GaBi J.*, **2**, 60 (2013); <https://doi.org/10.5639/gabij.2013.0202.022>
20. J. Griebinger, S. Dünnhaupt, B. Cattoz, P. Griffiths, S. Oh, S.B. Gómez, M. Wilcox, J. Pearson, M. Gumbleton, M. Abdulkarim, I.P. de Sousa and A. Bernkop-Schnürch, *Eur. J. Pharm. Biopharm.*, **96**, 464 (2015); <https://doi.org/10.1016/j.ejpb.2015.01.005>
21. S. Gurunathan, M.H. Kang, M. Qasim and J.H. Kim, *Int. J. Mol. Sci.*, **19**, 3264 (2018); <https://doi.org/10.3390/ijms19103264>
22. S. Hua, M.B.C. de Matos, J.M. Metselaar and G. Storm, *Front. Pharmacol.*, **9**, 790 (2018); <https://doi.org/10.3389/fphar.2018.00790>
23. L. Inchaurrega, N. Martín-Arbella, V. Zabaleta, G. Quincoces, I. Peñuelas and J.M. Irache, *Eur. J. Pharm. Biopharm.*, **97**, 280 (2015); <https://doi.org/10.1016/j.ejpb.2014.12.021>
24. L. Inchaurrega, A.L. Martínez-López, N. Martín-Arbella and J.M. Irache, *Drug Deliv. Transl. Res.*, **10**, 1601 (2020); <https://doi.org/10.1007/s13346-020-00796-3>
25. S. Thakur and G.K. Mohan, *BioNanoSci.*, **12**, 670 (2022); <https://doi.org/10.1007/s12668-022-00962-6>

26. F. Laffleur, F. Hintzen, G. Shahnaz, D. Rahmat, K. Leithner and A. Bernkop-Schnürch, *Nanomedicine*, **9**, 387 (2014); <https://doi.org/10.2217/nnm.13.26>
27. G.M. Morris, R. Huey, W. Lindstrom, M.F. Sanner, R.K. Belew, D.S. Goodsell and A.J. Olson, *J. Comput. Chem.*, **30**, 2785 (2009); <https://doi.org/10.1002/jcc.21256>
28. F. Cheng, W. Li, Y. Zhou, J. Shen, Z. Wu, G. Liu, P.W. Lee and Y. Tang, *J. Chem. Inf. Model.*, **52**, 3099 (2012); <https://doi.org/10.1021/ci300367a>
29. M.N. Drwal, P. Banerjee, M. Dunkel, M.R. Wettig and R. Preissner, *Nucleic Acids Res.*, **42**, W53 (2014); <https://doi.org/10.1093/nar/gku401>
30. A.A. D'souza and R. Shegokar, *Expert Opin. Drug Deliv.*, **13**, 1257 (2016); <https://doi.org/10.1080/17425247.2016.1182485>
31. S. Doktorovova, R. Shegokar, P. Martins-Lopes, A.M. Silva, C.M. Lopes, R.H. Müller and E.B. Souto, *Eur. J. Pharm. Sci.*, **45**, 606 (2012); <https://doi.org/10.1016/j.ejps.2011.12.016>
32. A. Kumar, S. Sharma, S. Mishra, S. Ojha and P. Upadhyay, *Anti-cancer Agents Med. Chem.*, **23**, 1499 (2023); <https://doi.org/10.2174/1871520623666230417080437>
33. O. Pechanova, A. Barta, M. Koneracka, V. Zavisova, M. Kubovcikova, J. Klimentova, J. Torok, A. Zemancikov and M. Cebova, *Molecules*, **24**, 2710 (2019); <https://doi.org/10.3390/molecules24152710>
34. S. Al-Zahrani, S. Astudillo-Calderón, B. Pintos, R. Pérez-Urria, J.A. Manzanera, L. Martín and A. Gomez-Garay, *Plants*, **10**, 1671 (2021); <https://doi.org/10.3390/plants10081671>
35. A.Z.M. Fahim, M.S. Ghouse, S.Q. Islam, M.A.M. Danish, S. Mehmood, S. Saniya and Q.I. Fatima, *Asian J. Pharm. Anal.*, **11**, 98 (2021); <https://doi.org/10.52711/2231-5675.2021.00018>
36. K. Maisel, M. Reddy, Q. Xu, S. Chattopadhyay, R. Cone, L.M. Ensign and J. Hanes, *Nanomedicine*, **11**, 1337 (2016); <https://doi.org/10.2217/nnm-2016-0047>
37. S.S. D'Souza and P.P. DeLuca, *Pharm. Res.*, **23**, 460 (2006); <https://doi.org/10.1007/s11095-005-9397-8>
38. S. Modi and B.D. Anderson, *Mol. Pharm.*, **10**, 3076 (2013); <https://doi.org/10.1021/mp400154a>
39. M. Yu, W. Yuan, D. Li, A. Schwendeman and S.P. Schwendeman, *J. Control. Release*, **315**, 23 (2019); <https://doi.org/10.1016/j.jconrel.2019.09.016>
40. Y. Zambito, E. Pedreschi and G. Di Colo, *Int. J. Pharm.*, **434**, 28 (2012); <https://doi.org/10.1016/j.ijpharm.2012.05.020>
41. M. Cetin, A. Atila and Y. Kadioglu, *AAPS PharmSciTech*, **11**, 1250 (2010); <https://doi.org/10.1208/s12249-010-9489-6>
42. J. Liu, D.A. Sonshine, S. Shervani and R.H. Hurt, *ACS Nano*, **4**, 6903 (2010); <https://doi.org/10.1021/nn102272n>